J. Coat. Technol. Res.
DOI 10.1007/s11998-009-9213-1

Morphology and corrosion resistance of Cr(III)-based conversion treatments for electrogalvanized steel

C. R. Tomachuk, C. I. Elsner, A. R. Di Sarli, O. B. Ferraz

Abstract The effectiveness of Cr(VI)-based passivation treatments is well accepted but there are many problems with regard to their environmental suitability. Because these compounds are carcinogenic and toxic, eco-friendly systems capable of replacing them are being evaluated. In this work, the corrosion behavior in 0.5 M NaCl solution of zinc coatings deposited from a free-cyanide alkaline bath and treated with Cr^{3+} based passivation coatings were characterized through DC and EIS techniques. The salt spray test as well as studies of the surface structure and chemical composition were also performed. From these analyses it was inferred that (1) the green-colored Cr^{3+} passivated coatings provide better corrosion resistance than the yellow- and blue-colored coatings, and (2) together with an adequate painting system, they could be a less polluting and less toxic alternative to traditional chromate coatings.

Keywords Conversion treatment, Corrosion, Green technologies, Impedance spectroscopy, Salt spray, Zinc

C. R. Tomachuk, O. B. Ferraz
Corrosion and Degradation Division, National Institute of Technology, Av. Venezuela, 82 sala 608, CEP 20081-312 Río de Janeiro, RJ, Brazil

C. R. Tomachuk
e-mail: tomachuk@br.surtec.com

C. I. Elsner, A. R. Di Sarli (✉)
CIDEPINT, Research and Development Center in Paint Technology (CIC-CONICET - La Plata), Av. 52 s/n entre 121 y 122, CP B1900AYB La Plata, Argentina
e-mail: direccion@cidepint.gov.ar; ardisarli@ciudad.com.ar

Introduction

Electroplated zinc coating is employed as an active galvanic protection for steel. However, as the zinc is an electrochemically high reactive metal, its corrosion rate may be high indoors, but *particularly* high under outdoor exposure conditions.[1] For this reason, it is necessary to have a post-treatment in order to increase the lifetime of zinc coatings. In current industrial practice, this treatment consists of immersion in a chemical bath that forms a conversion layer on the plated zinc. This latter layer is not only dielectrically passivated, but also has high corrosion resistance and offers a better surface for paint adherence. The main problem with traditionally used post-treatments is the presence of Cr^{6+} salts, considered carcinogenic substances, whose usage is forbidden by European norms.[2] Chromium-like compounds such as molybdates, tungstates, permanganates, and vanadates were the first chemical elements tried as substitutes for hexavalent chromium.[3–8] Recently, many alternative coatings were developed based on the zirconium and titanium salts,[9–11] cobalt salts,[12,13] organic polymers,[12,14–16] rare earth salts,[17–19] silane,[20,21] and carboxyl.[22] However, the corrosion behavior of these coatings is not clear and the practical usage of most of them is doubtful. A further possibility is the use of pretreatments based on trivalent chromium, which is not considered carcinogenic[23] and acts as a barrier (similar to hexavalent chromium).

The conversion treatment composition and morphology are very important for corrosion protection. Corrosion in green and yellow chromate coatings starts and propagates at the bottom of their cracked areas.[24] The cracks in the chromate coatings are attributable to the tensile stress in the coatings, which increases with the chromate layer thickness.[25] On the other hand, it was also reported that although chromate coatings have cracks, excellent corrosion protection could still be found, probably due to the coatings' composition.[24,26,27]

Published online: 11 September 2009

The length and size of cracks per unit area increase with dipping times in the chromate bath.[26]

In order to find an alternative treatment to Cr^{6+} conversion coating, several treatments that present good anti-corrosive behavior, high benefit/cost ratio and, especially, low environmental impact need to be developed. Usually, the coatings corrosion behavior is evaluated using traditional tests such as salt spray,[28] Kesternich,[29] and saturated humidity.[30] Nevertheless, the electrochemical methods used to obtain fast information about the corrosion reaction kinetics are also an important complimentary tool to take into account. Among the useful electrochemical techniques, the electrochemical impedance spectroscopy (EIS) was chosen based on the results obtained by others for metal and metal-coated corrosion evaluation.[31–34] As well, polarization measurements were also used to collect more information related to the corrosion processes developing on the different replicates subjected to the testing conditions later presented.

The main purpose of the work is to find an environmentally friendly conversion treatment that can be used for replacing the Cr^{6+} conversion treatment. Electrogalvanized steel covered with alternative treatments, free of Cr^{6+} ions, were investigated through AC and DC electrochemical techniques. The EIS data were fitted and interpreted by means of equivalent electrical circuit models. Chemical composition and morphological studies on the coatings' surfaces were also performed.

Experimental details

Samples preparation

AISI 1010 steel sheets (7.5 × 10 × 0.1 cm) were industrially electrogalvanized using a cyanide-free alkaline bath containing Zn^{2+} 10–12 g L^{-1}, NaOH 130–140 g L^{-1}, and commercial addition agents (temperature 25°C, cathodic current density 2 A dm^{-2}). Immediately after finishing the zinc deposition step, each sample was coated with the make-up described in Table 1, according to the operating conditions recommended by the supplier. At the end of this step, samples were again rinsed with deionized water and then dried.

Thickness measurements

Coating thickness was measured with a Helmut Fischer DUALSCOPE MP40, according to ASTM B499:1996 (2002).

Quali-quantitative chemical analyses and morphology

Coatings morphology was observed by SEM using a LEO 440i microscope, while the composition was determined using energy dispersive X-ray spectroscopy (EDXS).

Table 1: Coating films and operating conditions

Parameter	Sample		
	UF	UY	Z80
Make-up, % v/v			
Cr	0.02	0.03	0.14
S	0.02	–	–
Zn	Rest	Rest	Rest
Co	–	–	0.02
pH	1.9	1.8	1.6–2.1
Bath temperature (°C)	25	25	60
Immersion time (s)	30	30	60
Agitation	Mechanical		
Activation	0.5% HNO_3 solution for 10 s and then rinsed in deionized water		
Film color	Blue	Yellow	Green iridescent
Total coating thickness (μm)	16.00 ± 2.75	12.80 ± 0.37	10.4 ± 1.43

UF = passivation treatment = UniFix Zn-3-50 (LABRITS®); UY = passivation treatment = UniYellow 3 (LABRITS®); Z80 = passivation treatment = SurTec S680®

Electrochemical and corrosion behavior

The electrochemical cell consisted of a classic three-electrode arrangement; where the counter electrode (CE) was a platinum sheet, the reference electrode (RE) was a saturated calomel electrode (SCE = +0.244 V vs NHE), and the coated steel samples, with a defined area of 15.9 cm^2, acted as the working electrode (WE). All measurements were performed at a constant room temperature (22 ± 3°C) in 0.5 M NaCl solution.

Potentiodynamic polarization experiments were carried out using a Solartron 1280 electrochemical system at a sweep rate of 0.2 mV s^{-1}, over the range ±0.250 V(SCE) with respect to the open-circuit potential (OCP). The electrodes were stabilized for several minutes in the solution before starting each test.

Impedance spectra in the frequency range 10^{-3} Hz < f < 10^5 Hz were performed in the potentiostatic mode at the open circuit potential, as a function of the exposure time in the electrolyte solution, using a Solartron 1255 Frequency Response Analyzer (FRA) coupled to a Solartron 1286 electrochemical interface (EI) and controlled by the ZPlot program from Scribner Associates Inc. A sinusoidal signal with amplitude of 15 mV was applied and 10 points per decade were registered. The corrosion behavior was analyzed until white corrosion products on the

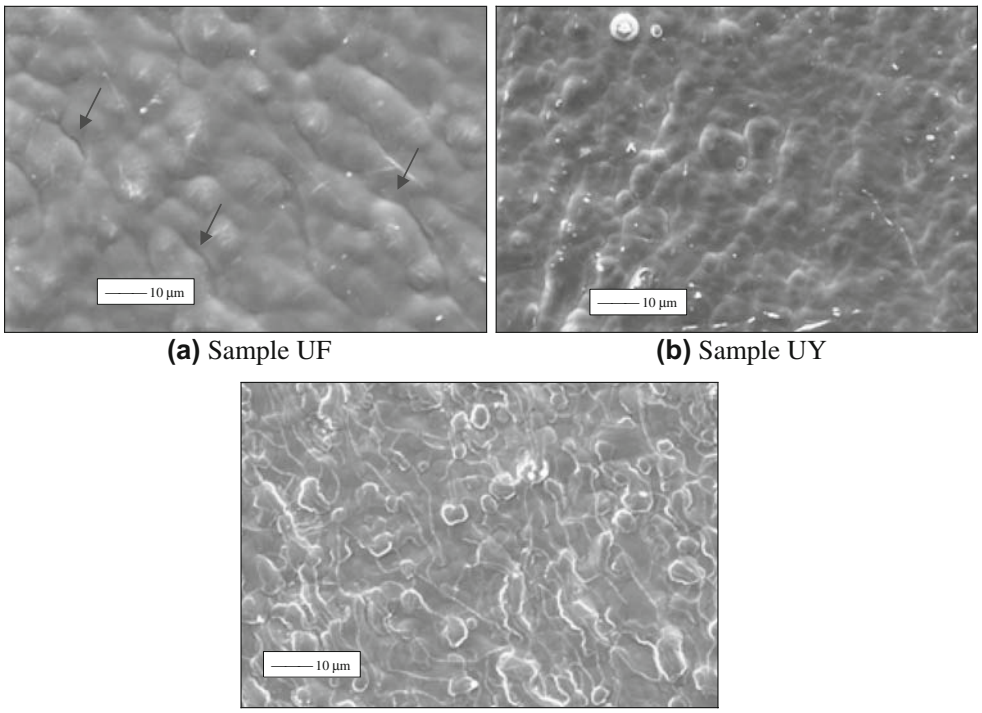

(a) Sample UF **(b)** Sample UY

(c) Sample Z80

Fig. 1: Microstructure of the tested coatings

samples' surface could be seen by the naked eye. The experimental spectra were fitted and interpreted on the basis of equivalent electrical circuits using software (EQUIVCRT) developed by Boukamp.[35] All impedance measurements were performed with the electrochemical cell inside a Faraday cage to reduce external interferences as much as possible.

The coatings' corrosion resistance was also studied by exposing replicates of the samples in a salt spray chamber in accordance with ASTM B117:2002 (5% NaCl, T = 35°C). The surface percentage covered with red rust was evaluated at various exposure times using the ASTM D-610 standard.

In order to improve the experimental data reproducibility in each one of the above-mentioned tests, three replicates of each pre-treated specimen were chosen after characterizing their surface parameters.

Results and discussion

The identification symbol, chemical composition, and overall coating thickness of the tested samples are summarized in Table 1, where the reported variation of the average coating thickness values was attributed to the measurement error as well as to the fact that the galvanized steel sheets were produced, and the conversion layer applied, under operating conditions of a continuous galvanizing line, where these types of variations are commonly found. The average thickness of UF samples was higher than in UY and Z80 samples. Unfortunately, information related to the specific thickness of the conversion layers was not possible to obtain. With regard to other surface characteristics, all of them were uniform and bright.

Table 1 also shows that results provided by the surface coating analyses, made by EDXS, revealed the presence of mainly Cr, Zn, S (in UF samples), and Co (in Z80 samples). Cobalt ions added to these last samples suggest an improvement in its corrosion resistance,[36] while the presence of sulfur in UY samples was probably related to the sulphate ions contained in the treatment bath.

Morphology

After the conversion treatment, the surface morphology of the coatings was observed at up to 1000× by SEM (Fig. 1). All the samples showed rough surfaces. Likewise, UF samples (Fig. 1a) exhibited few surface fissures (indicated by the black arrows), which reduce its protective properties, while the UY samples (Fig. 1b) showed homogenous structure with nodular growth and small fissures. On the other hand, perhaps because of its gel-like structure and lower thickness, Z80 samples (Fig. 1c) did not present the crack-networks characteristic of chromate coatings.[24]

Electrochemical behavior

Polarization curves

Potentiodynamic polarization curves were performed for all the investigated samples. Figure 2 shows typical curves obtained for passivated electrogalvanized steel in contact with a chloride-containing solution.

From current density/electrode potential data obtained in the potential range OCP ± 0.250 mV, the corrosion current density values (j_{corr}) were determined from the Tafel line extrapolation of the anodic j–E curve to the corrosion potential.[37] The j_{corr} and E_{corr} data are summarized in Table 2.

As it can be seen, UY and Z80 samples present a similar and nobler corrosion potential value than UF samples, indicating a thermodynamic improvement in corrosion resistance as well as a better barrier behavior, probably due to the homogenous morphology of their covering layer as shown in Figs. 1b and 1c. On the other hand, the corrosion current density (j_{corr}) of Z80 samples is at least one order of magnitude less than those corresponding to the other samples. Such a decrease in the corrosion rate is attributable to the effective inhibitive action afforded by the Co added to the passive layer.[36]

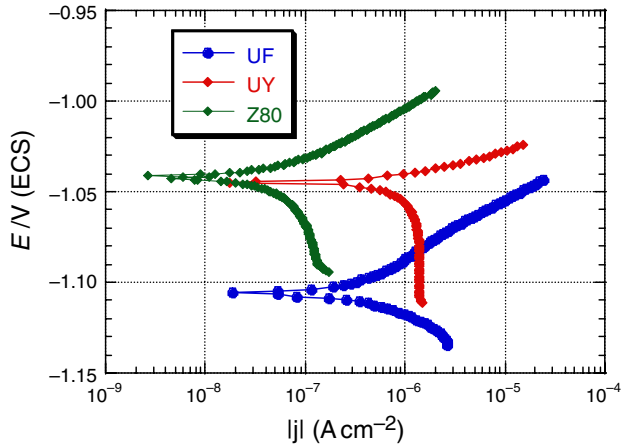

Fig. 2: Polarization curves of UF, UY, and Z80 samples in 0.5 M NaCl solution

Table 2: E_{corr} and j_{corr} values of Zn coatings after applying the conversion treatment

Identification	E_{corr} V(SCE)	j_{corr} (μA/cm^2)
UF	−1.11	0.09
UY	−1.04	0.30
Z80	−1.04	0.02

EIS measurements

EIS measurements were carried out at room temperature in NaCl 0.5 M solution until the appearance of macroscopic white corrosion products on the sample surfaces.

Representative Bode (impedance modulus and phase angle vs frequency) plots as a function of the exposure time in 0.5 M NaCl solution are presented for UF (Figs. 3a and 3b), UY (Figs. 4a and 4b), and Z80 samples (Figs. 5a and 5b), where (a) represents short immersion times (up to 24 h) and (b) long immersion times. The electrical equivalent circuit used for fitting such data is depicted in Fig. 6.

SHORT IMMERSION TIMES: At low frequencies, it was observed that Z80 samples exhibit higher initial $|Z|$ values than UF and UY samples. This behavior is in agreement with the results obtained from polarization curves and confirms that the corrosion protection provided by the Z80 conversion treatment is also more effective due to its more compact coating structure. After 60 min of exposure, the Z80 impedance values at medium and low frequencies decreased approximately one order of magnitude and remained at $\sim 10^3\ \Omega\ cm^2$, suggesting an electrochemically active interface.

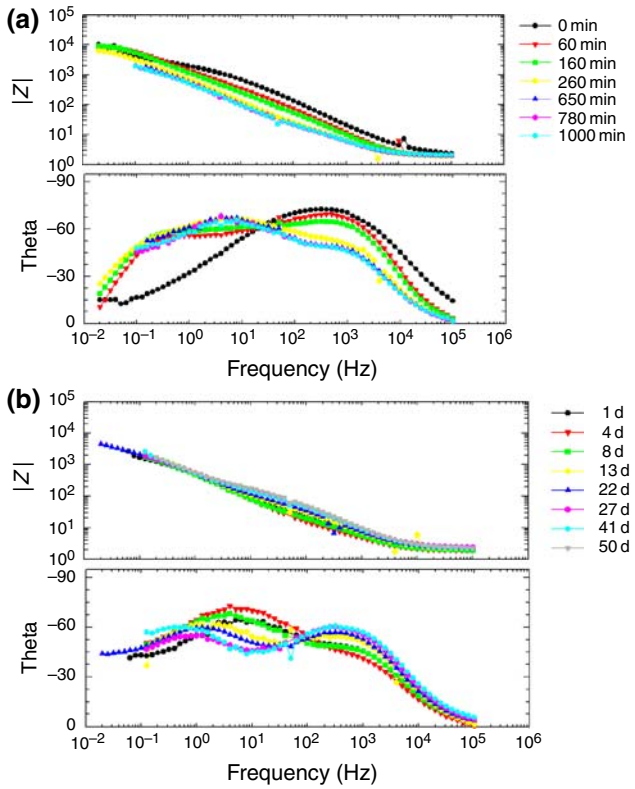

Fig. 3: Time dependence of UF samples impedance at short (a) and long (b) immersion period in 0.5 M NaCl solution

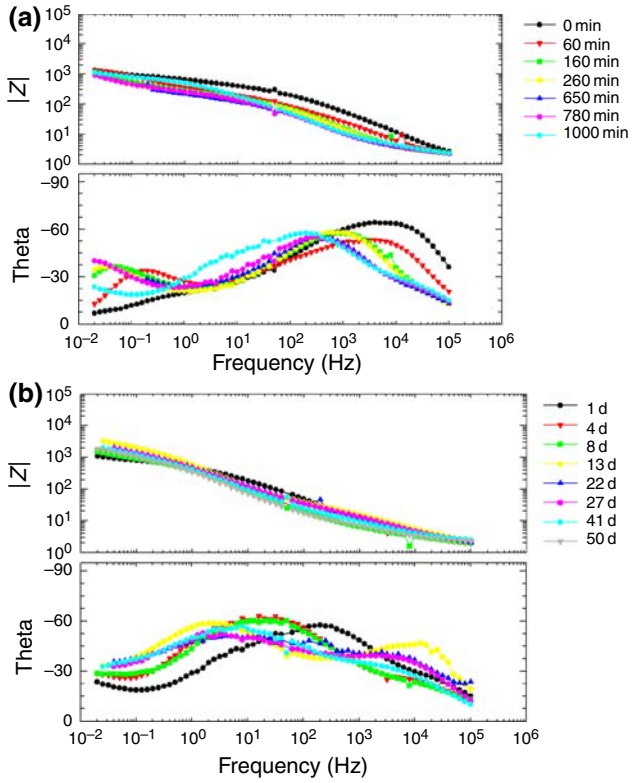

Fig. 4: Time dependence of UY samples' impedance at short (a) and long (b) immersion period in 0.5 M NaCl solution

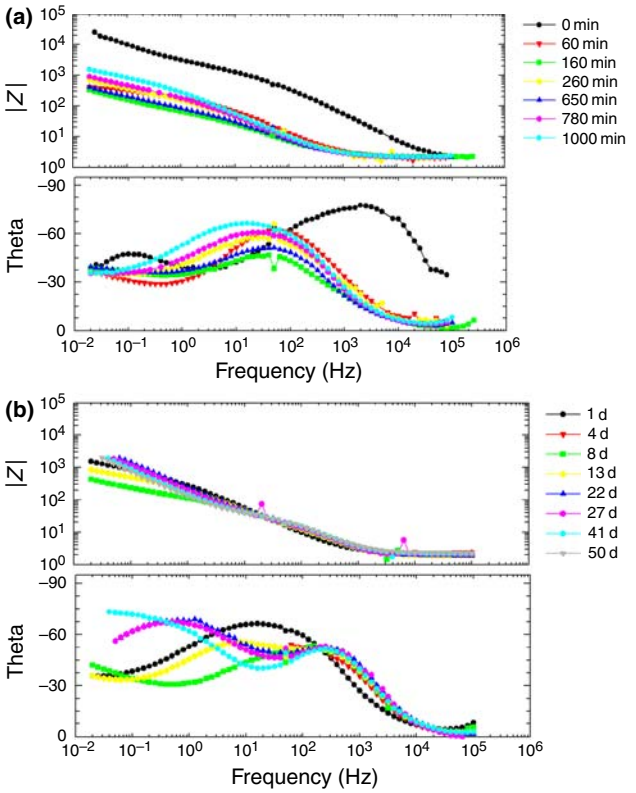

Fig. 5: Time dependence of Z80 samples' impedance at short (a) and long (b) immersion period in 0.5 M NaCl solution

Likewise, the impedance module values at high frequencies, which are related to the barrier resistance of the conversion coating, showed a fast decrease that was related to the dissolution of this thin protective layer.

By comparing UF and UY samples' performance, the slightly higher impedance values of UF samples was in agreement with the small difference in corrosion rates between the two as observed in Fig. 2. In addition, changes in phase-angle values observed along the entire range of frequencies suggest an active mechanism of dissolution–passivation at the conversion layer/zinc interface during the first steps of exposure to the aggressive solution. This assumption is confirmed by the appearance of two or more time constants after 60 min exposure, and it can be related to the presence of fissures in the conversion layer (Figs. 1a and 1b).

LONG IMMERSION TIMES: As seen in Figs. 3a and 3b, the main changes in UF samples took place during the first day of immersion in the NaCl solution. Latterly, the impedance module values at low frequencies, about 10^3–10^4 Ω cm^2, are evidence of certain electrochemical activity at the conversion treatment/zinc interface. This behavior indicates that the zinc film thickness plays an important role in corrosion protection when long immersion times must be planned. A similar performance was shown by UY (Fig. 4b) and Z80 samples (Fig. 5b), but with impedance module values ranging from 10^2 to 10^3 Ω cm^2.

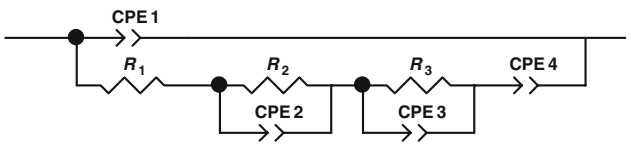

Fig. 6: Equivalent circuit used to model the impedance data of UF, UY, and Z80 samples submerged in 0.5 M NaCl solution

In all the samples, changes in phase angle values observed over the entire range of frequencies also suggest an active mechanism of dissolution–passivation at the conversion layer/zinc interface during long exposure to the aggressive solution. In this sense, the displacement of the point at which the phase angle reaches its maximum value toward lower frequencies indicates the continuous deterioration of the passive layer protection and, consequently, the development of a faster corrosion processes.

One of the more important difficulties for analyzing the electrochemical impedance data from the impedance spectra deconvolution is, in general, to find an electrical equivalent circuit model and/or the

parameters needed to explain the corrosion behavior of each analyzed system. In this paper, the equivalent circuit model that allowed the description of the time exposure dependence of such behavior in steel/zinc coating/conversion layer/aqueous electrolyte systems is shown in Fig. 6. In the figure, the first time constant (R_1CPE$_1$) appeared at the higher frequencies and represents the resistance to the ionic flux (R_1) and the dielectric capacitance (CPE$_1$) of the conversion layer. As the frequency values diminished, and taking into account that the permeating and corrosion-inducing chemicals (water, oxygen, and ionic species) reach the electrochemically active areas of the substrate through the coating pores characterized by R_1, it is reasonable to assume the corrosion process developing at the zinc surface should be placed in series with R_1. The R_2 and CPE$_2$ parameters account for the charge transfer resistance and the electrochemical double layer capacitance of the corrosion process, respectively. As a result of the zinc dissolution, corrosion products accumulate at the bottom of the pores. Their contribution to the system impedance is characterized by the R_3 and CPE$_3$ parameters.[37–40] The diffusional component Z_d obtained at certain exposure times was associated with an oxygen diffusion-controlled reaction usually found in zinc corrosion.[41,42,43]

All the time constants exhibited some Cole-Cole type dispersion which had the corresponding n_i parameter, being $0 < n_i \leq 1$. Furthermore, distortions observed in those resistive-capacitive contributions indicate a deviation from the theoretical models in terms of a time constants distribution due to either lateral penetration of the electrolyte at the metal/coating interface (usually started at the base of intrinsic or artificial coating defects), underlying metallic surface heterogeneity (topological, chemical composition, surface energy), and/or diffusional processes that could take place along the test. Since all these factors cause the impedance/frequency relationship to be non-linear, they are taken into consideration by replacing one or more capacitive components (C_i) of the equivalent circuit transfer function by the corresponding constant phase element (CPE), for which the impedance may be expressed as[44–46]:

$$Z = \frac{(j\omega)^{-n}}{Y_0}$$

where $Z(\omega)$ is the impedance of the CPE ($Z = Z' + jZ''$) (Ω), J is the imaginary number ($j^2 = -1$), ω is the angular frequency (rad), n is the CPE power ($n = \alpha/(\pi/2)$, α is the constant phase angle of the CPE (rad), and Y_0 is the part of the CPE independent of the frequency (Ω^{-1}).

Difficulties are sometimes found in providing an accurate physical description of the occurred processes. In such cases, a standard deviation (χ^2) $\leq 5 \times 10^{-4}$ was used as final criterion by considering that the smaller this value is, the closer the fit is to the experimental data.[35] In the present work, the fitting process was mainly performed using the phase constant element (CPE$_i$) instead of the dielectric capacitance C_i. However, this last parameter was used in the following plots in order to facilitate the results visualization and interpretation.

The R_1, C_1, R_2, C_2, R_3, C_3, and Z_d parameter values estimated from the impedance spectra fitting analysis at short and long exposure times are respectively reported in Figs. 7a–7g and 8a–8g.

Time dependence of the impedance resistive and capacitive components

Short exposure time: As already mentioned, being used without any other type of protection, the extremely poor barrier properties provided by the conversion layer made it possible for the zinc corrosion reaction initiated just after immersion in the NaCl solution. This fact is denoted by the oscillating R_1 values in the ranges 10^2–10^3 Ω cm^2 (UF and UY samples), 10^3–10^5 Ω cm^2 (Z80 samples), and also by the low values, 10^{-6}–10^{-4} F cm^{-2} (UY and Z80 samples) and 5.10^{-5}–10^{-3} F cm^{-2} (UF samples) of the dielectric capacitance (C_1) coupled to the ionic flux resistance (Figs. 7a and 7b).

Similarly, the evolution of the parameters associated with the zinc dissolution (R_2, C_2) and corrosion products development (R_3, C_3) (Figs. 7c–7f) reflects that the increase of pathways through the conversion layer for the electrolyte to reach the zinc film favors not only the Cl^- reaction with this metal, and hence the protective coating degradation, but also the accumulation of corrosion products at the bottom of the pores. After a certain induction period, the volume of these products is high enough to act like a barrier delaying the oxygen diffusion towards cathodic reaction areas (Fig. 7g). Such behavior can often cause the process controlling the corrosion-rate determining step to change from activated to mass transport or a mixture of the two. At the same time, the electrochemically active area is being modified, and this led to the observed fluctuating movement of the resistive and capacitive components of the working electrode impedance. In order to explain this performance, it was assumed that the white rust either continuously dissolved and/or eventually detached from the substrate.[47,48] The time dependence of all these parameters showed in Figs. 7a–7g suggests that although with kinetics defined by the surface topography and chemical composition of each sample, the superficial condition of Z80, UF, and UY samples changed continuously and dynamically from the beginning up to 1000-min immersion.

Long exposure time: As time went on, the behavior differences found at short exposure times in NaCl solution for Z80, UF, and UY samples became less

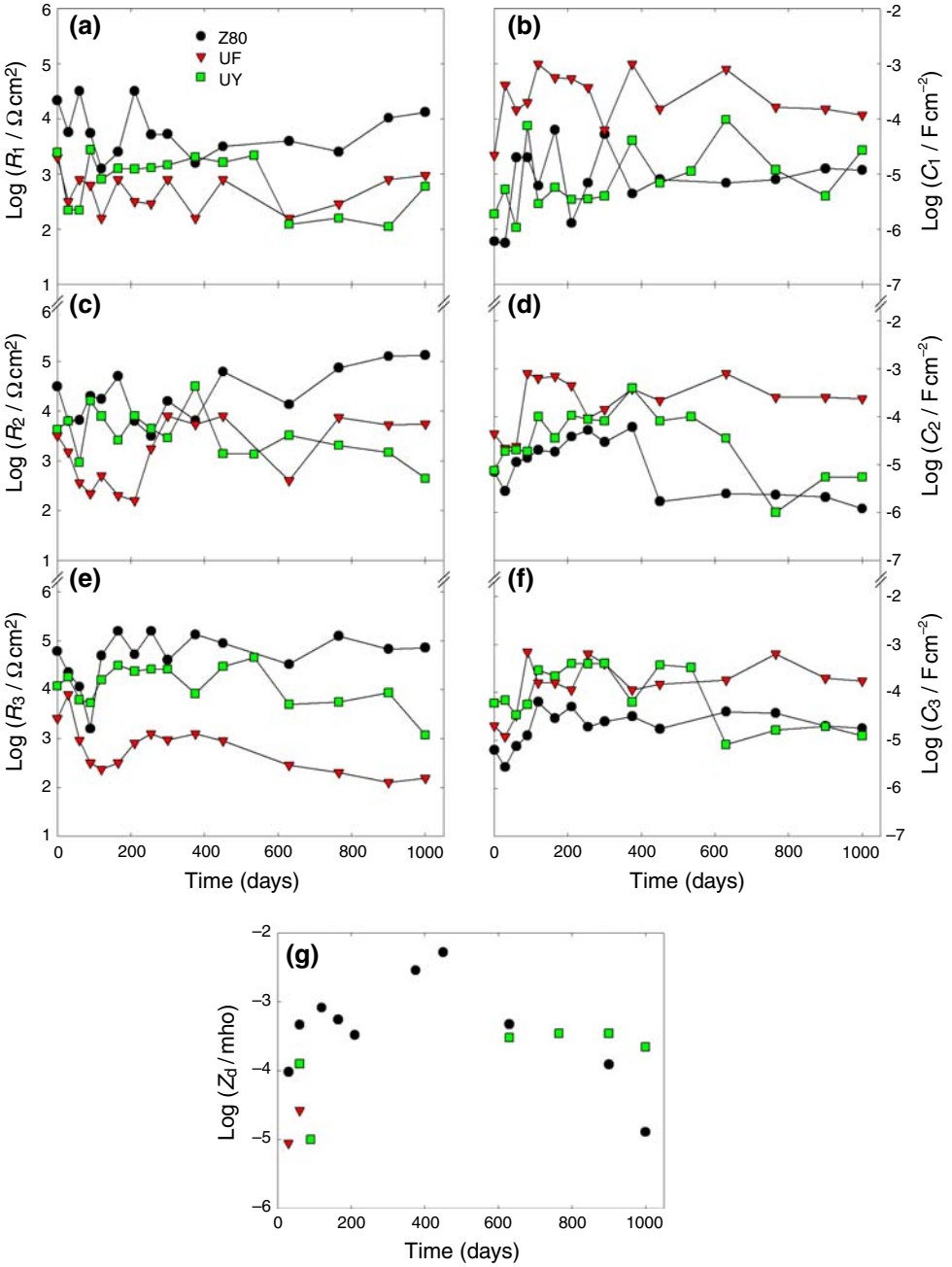

Fig. 7: Evolution of (a) log R_1, (b) log R_2, (c) log R_3, (d) log C_1, (e) log C_2, (f) log C_3, and (g) log Z_d parameters of all the tested specimens at short exposure times in 0.5 M NaCl solution

significant (Figs. 8a–8g). Nevertheless, the number of time constants deconvoluted from the impedance spectra remained unchanged. Again, the worst protective performance was showed by UF samples, whose test was ended at 42-day exposure due to the high and uniform degradation exhibited throughout all the surface. In addition, mass transport control, as the rate-determining step of the zinc corrosion reaction, was found at zero immersion time, i.e., the high corrosion rate was always under activated control (zinc dissolution) probably due to the Cr(III) in the conversion layer being too low (0.02%) to provide any type of anticorrosive protection to the zinc substrate.

In agreement with the results obtained through the other tests performed in the present work, the conversion layer applied in Z80 samples offered the best protective properties against the attack of the underlying zinc layer by, in this case, aqueous aggressive medium containing a high Cl^- ion concentration. In terms of such a performance, it was followed by UY samples. The assumptions made for explaining these results have been explained in previous paragraphs;

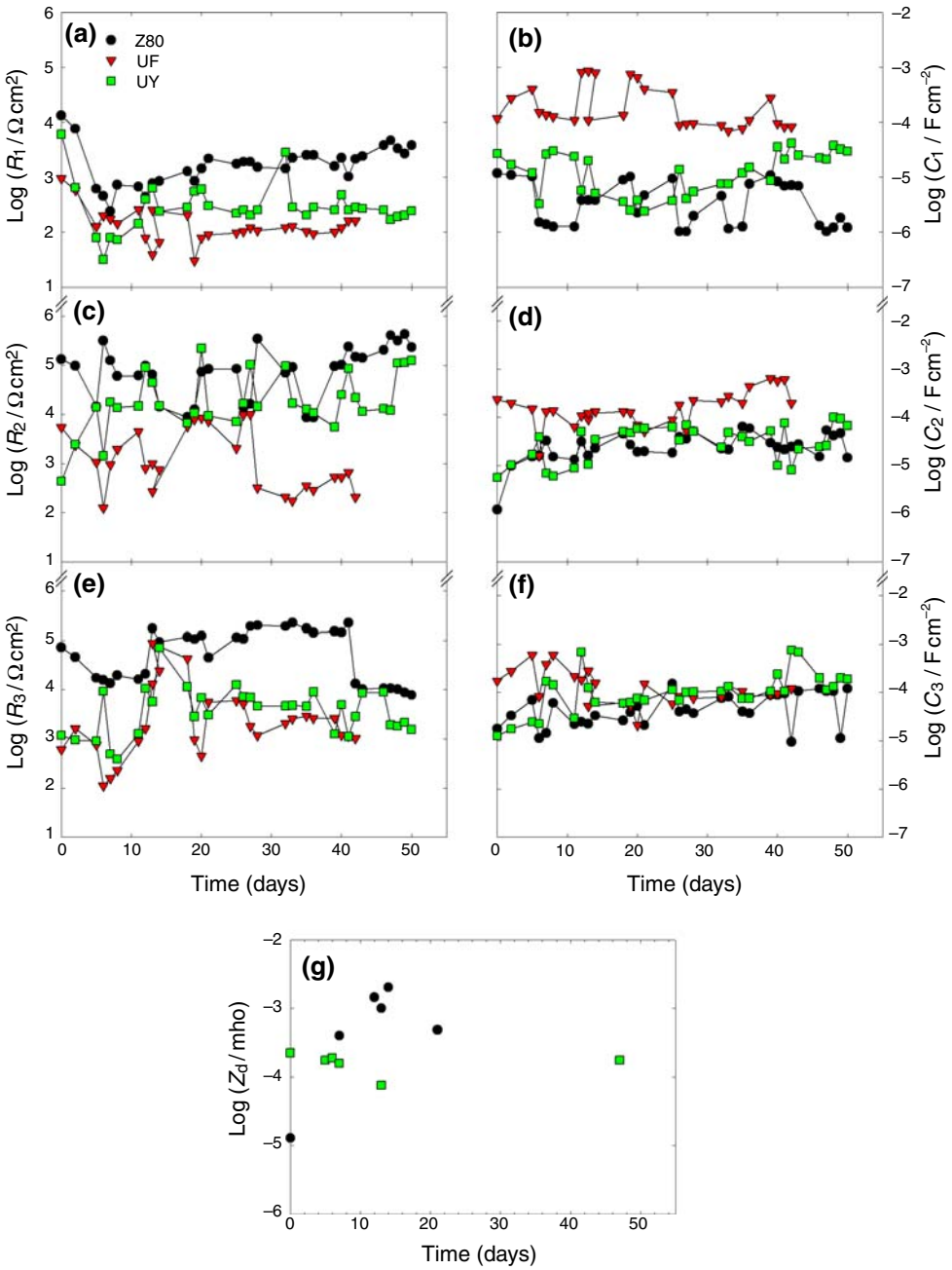

Fig. 8: Evolution of (a) log R_1, (b) log R_2, (c) log R_3, (d) log C_1, (e) log C_2, (f) log C_3, and (g) log Z_d parameters of all the tested specimens at long exposure times in 0.5 M NaCl solution

however, it can be added that after certain exposure time has elapsed, the value of the impedance components of both sample types showed a trend to be closer and stabilized.

Salt spray test

Salt spray tests were conducted with Z80, UF, and UY samples. They were discontinued upon visual observation of red corrosion products on the surface. It is important to note that the protective performance of the coating passivation layer strongly depends on its chemical composition and application parameters. This is to say, as the coating Cr(III) content, thickness and continuity increase, higher and longer corrosion protection is expected.

The surface degradation percentage vs exposure time after the salt spray test for all the samples is shown in Fig. 9. In this figure it can be seen that the surface degradation of UF samples started earlier (at ~40 h exposure) and increased very fast, reaching

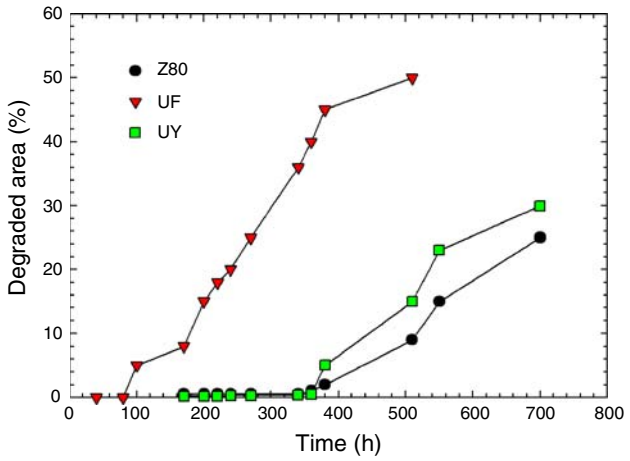

Fig. 9: Surface damage during salt spray test

~50% at 500 h exposure. In UY and Z80 samples, the process initiated at 170 and 190 h, respectively, but its development was significant after 380 h. Such a behavior suggests that the coating corrosion resistance is directly related to the chromium content in the conversion layer. These results are in good agreement with EIS measurements and polarization curves.

Conclusions

Results derived from the study allowed us to infer the following conclusions:

- The presence of fissures in the UF and UY conversion layers creates fast pathways for the electrolytes to reach the zinc substrate, leading to its quick dissolution.
- The more important changes, shown by the impedance spectra, took place after 60 min exposure to the electrolyte. Such changes were greater for samples Z80 even though they showed the best anticorrosive behavior at increasing exposure times.
- Surface analyses, used together with electrochemical techniques, proved to be a very useful tool to characterize the alternative conversion treatments and their results were in good agreement with those obtained from the salt spray test. By comparing all of these experimental results, it was clear that Z80 samples presented lower corrosion rates than UY and UF samples. This behavior was attributed to the coatings' higher Cr(III) content, thickness, and continuity.
- The investigated conversion treatments, based on Cr(III), seem to be an interesting alternative to those using Cr(VI). However, the authors think that other experiments need to be performed in order to evaluate their effectiveness when they form part of specific painting schemes.

Acknowledgments The authors acknowledge FAPERJ (Process E-26/152.259/2003), FINEP (Process n. 22.01.0752.00) of Brazil, and Comisión de Investigaciones Científicas de la Provincia de Buenos Aires (CIC) and Consejo Nacional de Investigaciones Científicas y Técnicas (CONICET) of Argentina for their financial support to this research, and IPT, of Brazil, for preparing the samples.

References

1. Zaki, N, "Chromate Conversion Coating for Zinc." *Met. Finish.*, **86** (2) 75–76 (1988)
2. Hagans, PL, Haas, CM, *ASM Handbook Surface Engineering*, p. 405, Vol. 5 (1994)
3. Almeida, E, Diamantino, TC, Figueiredo, MO, Sá, C, "Oxidizing Alternative Species to Chromium VI in Zinc Galvanized Steel Surface Treatment. Part 1—A Morphological and Chemical Study." *Surf. Coat. Technol.*, **106** 8–17 (1998)
4. Almeida, E, Fedrizzi, L, Diamantino, TC, "Oxidizing Alternative Species to Chromium VI in Zinc-Galvanized Steel Surface Treatment. Part 2—An Electrochemical Study." *Surf. Coat. Technol.*, **105** 97–101 (1998)
5. Wilcox, GD, Gabe, DR, "Passivation Studies Using Group VIA Anions. Part 5: Cathodic Treatment of Zinc." *Br. Corr. J.*, **22** (4) 254–256 (1987)
6. Wilcox, GD, Gabe, DR, Warwick, ME, "The Development of Passivation Coatings by Cathodic Reduction in Sodium Molybdate Solutions." *Corros. Sci.*, **28** 577–587 (1988)
7. Korobov, VI, Loshkarev, YM, Kozhura, OV, "Cathodic Treatment of Galvanic Zinc Coatings in Solutions of Molybdates." *Russ. J. Electrochem.*, **34** (11) 1154–1157 (1998)
8. Magalhães, AAO, Margarit, ICP, Mattos, OR, "Molybdate Conversion Coatings on Zinc Surfaces." *J. Electrochem. Chem.*, **572** (2) 433–440 (2004)
9. Deck, PD, Reichgott, DM, "Characterization of Chromium-Free No-Rinse Prepaint Coating on Aluminum and Galvanized Steel." *Met. Finish.*, **9** (90) 29–35 (1992)
10. Hinton, BRW, "Corrosion Prevention and Chromates: The End of an Era?" *Met. Finish.*, **89** 55–61 (1991)
11. Hinton, BRW, "Corrosion Prevention and Chromates: The End of an Era?" *Met. Finish.*, **89** 15–20 (1991)
12. Barbucci, M, Delucchi, M, Cerisola, G, "Study of Chromate-Free Pretreatments and Primers for the Protection of Galvanized Steel Sheets." *Prog. Org. Coat.*, **33** (2) 131–138 (1998)
13. Wilcox, GD, Wharton, JA, "A Review of Chromate-Free Passivation Treatments for Zinc and Zinc Alloys." *Trans. IMF*, **75** (4) B140–B146 (1997)
14. Child, TF, *Revue Surface*, **280** 56–59 (1998)
15. González, S, Gil, MA, Hernández, JO, Fox, V, Souto, RM, "Resistance to Corrosion of Galvanized Steel Covered with an Epoxy-Polyamide Primer Coating." *Prog. Org. Coat.*, **41** (1–3) 167–170 (2001)
16. Duarte, RG, Bastos, AC, Castela, AS, Ferreira, MGS, "A Comparative Study Between Cr(VI)-Containing and Cr-Free Films for Coil Coating Systems." *Prog. Org. Coat.*, **52** (4) 320–327 (2005)
17. Montemor, MF, Simões, AM, Ferreira, MGS, Breslin, CB, "Composition and Corrosion Behavior of Galvanized Steel

Treated with Rare-Earth Salts: The Effect of the Cation.'' *Prog. Org. Coat.*, **44** (2) 111–120 (2002)
18. Trabelsi, W, Cecilio, P, Ferreira, MGS, Montemor, MF, ''Electrochemical Assessment of the Self-Healing Properties of Ce-Doped Silane Solutions for the Pre-treatment of Galvanized Steel Substrates.'' *Prog. Org. Coat.*, **54** (4) 276–284 (2005)
19. Johnson, BY, Edington, J, Williams, A, O'Keefe, MJ, ''Microstructural Characteristics of Cerium Oxide Conversion Coatings Obtained by Various Aqueous Deposition Methods.'' *Mater. Charact.*, **54** (1) 41–48 (2005)
20. Trabelsi, W, Triki, E, Dhouibi, L, Ferreira, MGS, Zheludkevich, ML, Montemor, MF, ''The Use of Pre-treatments Based on Doped Silane Solutions for Improved Corrosion Resistance of Galvanized Steel Substrates.'' *Surf. Coat. Technol.*, **200** (14–15) 4240–4250 (2006)
21. Ferreira, MGS, Duarte, RG, Montemor, MF, Simões, AMP, ''Silanes and Rare Earth Salts as Chromate Replacers for Pre-treatments on Galvanized Steel.'' *Electrochim. Acta*, **49** (17–18) 2927–2935 (2004)
22. Peultier, J, Rocca, E, Steinmetz, J, ''Zinc Carboxylating: A New Conversion Treatment of Zinc.'' *Corros. Sci.*, **45** (8) 1703–1716 (2003)
23. Bellezze, T, Roventi, G, Fratesi, R, ''Electrochemical Study on the Corrosion Resistance of Cr III-Based Conversion Layers on Zinc Coatings.'' *Surf. Coat. Technol.*, **155** (2–3) 221–230 (2002)
24. Martyah, NM, McCaskie, JE, Harrison, L, ''Corrosion Behavior of Zinc Chromate Coatings.'' *Met. Finish.*, **94** (2) 65–67 (1996)
25. Martyah, NM, ''Internal Stresses in Zinc-Chromate Coatings.'' *Surf. Coat. Technol.*, **88** (1–3) 139–146 (1996)
26. Zhang, X, van den Bos, C, Sllof, WG, Terryn, H, Hovestad, A, de Wit, JHW, ''Investigation of Cr(VI)- and Cr(III)-Based Conversion Coatings on Zinc.'' *J. Corros. Sci. Eng.*, **6** 1–57 (2003)
27. Zhang, X, Sloof, WG, Hovestad, A, van Westing, EPM, Terryn, H, de Wit, JHW, ''Characterization of Chromate Conversion Coatings on Zinc Using XPS and SKPFM.'' *Surf. Coat. Technol.*, **197** (2–3) 168–176 (2005)
28. Standard Practice for Operating Salt Spray (Fog) Apparatus, ASTM B117: 1993, p. 10 (1993)
29. Testing in a Saturated Atmosphere in the Presence of Sulphur Dioxide, DIN 50018, p. 6 (1997)
30. Atmospheres and Their Technical Application Condensation Water Test Atmospheres, DIN 50017, p. 10 (1982)
31. MacDonald, JR, *Impedance Spectroscopy Emphasizing Solid State Materials*. Wiley, New York (1987)
32. Mansfeld, F, ''Models for the Impedance Behavior of Protective Coatings and Cases of Localized Corrosion.'' *Electrochim. Acta*, **38** (14) 1891–1897 (1993)
33. Carbonini, P, Monetta, T, Nicodemo, L, Mastronardi, P, Scatteia, B, Bellucci, F, ''Electrochemical Characterization of Multilayer Organic Coatings.'' *Prog. Org. Coat.*, **29** (1–4) 13–20 (1996)
34. De Rosa, L, Monetta, T, Mitton, DB, Bellucci, F, ''Monitoring Degradation of Single and Multilayer Organic Coatings. I. Absorption and Transport of Water: Theoretical Analysis and Methods.'' *J. Electrochem. Soc.*, **145** (11) 3830–3838 (1998)
35. Boukamp, BA, *Equivalent Circuit*, Report CT88/265/128, CT89/214/128, University of Twente, The Netherlands (1989)
36. Fratesi, R, Roventi, G, Giuliani, G, Tomachuk, CR, ''Zinc–Cobalt Alloy Electrodeposition from Chloride Baths.'' *J. Appl. Electrochem.*, **27** (9) 1088–1094 (1997)
37. Dattilo, M, ''Polarization and Corrosion of Electrogalvanized Steel—Evaluation of Zinc Coatings Obtained from Waste-Derived Zinc Electrolytes.'' *J. Electrochem. Soc.*, **132** (11) 2557–2561 (1985)
38. Deflorian, F, Rossi, S, Fedrizzi, L, Bonora, PL, ''EIS Study of Organic Coating on Zinc Surface Pretreated with Environmentally Friendly Products.'' *Prog. Org. Coat.*, **52** (4) 271–279 (2005)
39. Fedrizzi, L, Claghl, L, Bonora, BL, Fratessi, R, Roventi, G, ''Corrosion Behavior of Electrogalvanized Steel in Sodium Chloride and Ammonium Sulphate Solutions; a study by E.I.S.'' *J. Appl. Electrochem.*, **22** (3) 247–254 (1992)
40. Rangel, CM, Cruz, LF, ''Zinc Dissolution in Lisbon Tap Water.'' *Corros. Sci.*, **33** (9) 1479–1493 (1992)
41. Cachet, C, Wiart, R, ''The Kinetics of Zinc Dissolution in Chloride Electrolytes: Impedance Measurements and Electrode Morphology.'' *J. Electroanal. Chem.*, **111** 235–246 (1980)
42. Cachet, C, Wiart, R, ''Reaction Mechanism for Zinc Dissolution in Chloride Electrolytes.'' *J. Electroanal. Chem.*, **129** 103–114 (1981)
43. Amirudin, A, Thierry, D, ''Application of Electrochemical Impedance Spectroscopy to Study the Degradation of Polymer-Coated Metals.'' *Prog. Org. Coat.*, **26** (1) 1–28 (1995)
44. Abreu, CM, Izquierdo, M, Keddam, M, Nóvoa, XR, Takenouti, H, ''Application of Electrochemical Impedance Spectroscopy to Study the Degradation of Polymer-Coated Metals.'' *Electrochim. Acta*, **41** (15) 2405–2415 (1996)
45. del Amo, B, Véleva, L, Di Sarli, AR, Elsner, CI, ''Performance of Coated Steel Systems Exposed to Different Media: Part I. Painted Galvanized Steel.'' *Prog. Org. Coat.*, **50** (3) 179–192 (2004)
46. van Westing, EPM, Ferrari, GM, Geenen, FM, de Wit, JHW, ''In Situ Determination of the Loss of Adhesion of Barrier Epoxy Coatings Using Electrochemical Impedance Spectroscopy.'' *Prog. Org. Coat.*, **23** (1) 89–103 (1993)
47. Shih, HC, Hsu, JW, Sun, CN, Chung, SC, ''The Lifetime Assessment of Hot-dip 5% Al–Zn Coatings in Chloride Environments.'' *Surf. Coat. Technol.*, **150** (1) 70–75 (2002)
48. Ahmed El-Mahdy, G, Nishikata, A, Tsuru, T, ''Electrochemical Corrosion Monitoring of Galvanized Steel Under Cyclic Wet–Dry Conditions.'' *Corros. Sci.*, **42** (1) 183–194 (2000)